Hybrid Model for Vertical Deflection Component Determination

Basil Daniel Devote and Lawrence Hart
Department of Surveying and Geomatics,
Faculty of Environmental Sciences, Rivers State University, Nigeria
basil.devote@ust.edu.ng

DOI: https://dx.doi.org/10.4314/sajg.v14i2.8

Abstract

Observations (horizontal and vertical angles, azimuth, and zenith distances) made by surveyors and geodesists in their quest to solve spatial problems in the mapping of the Earth's surface are carried out with respect to the Earth's gravity field (geoid). The irregularity and non-homogeneity of the Earth's mass-density distribution have made the geoidal surface unsuitable for the computation and adjustment of spatial data. Hence, the ellipsoid has been adopted as an approximation of the geoid surface for mathematical computation. The non-coincidence of the normal between these surfaces (the geoid and ellipsoid) underscores the criticality of the vertical deflection for reducing these observations to the ellipsoid. The need to provide a framework that will ensure the seamless transformation and conversion of the coordinates of varying reference surfaces (geoid and ellipsoid) and the reduction of astronomical quantities to the ellipsoid underscores the justification of this research. Hence, a hybrid model was developed to determine the vertical deflection component in Rivers State, Nigeria. This involved integrating geoid height differences from GPS/levelling with those from the global Earth Gravity Model (EGM 2008). Using the least squares method, the components of the deflection of the vertical for fifteen stations were calculated: they ranged from -0.0552" to 0.0784" in the north-south component and from -0.05940" to 0.21530" in the east-west component. The component of the deflection of the vertical computed using the various models gives values of ξ = 0.0473", η = -0.0393"; ξ = 0.0404", -0.0345"; ξ = 0.0157", η = 0.0157" for the geometric method, hybrid, and the EGM 2008 models, respectively. A map illustrating the deflection of the vertical for the study area was created, and a Graphical User Interface (GUI) was implemented to determine the deflection of the vertical at any location within the study area using the MATLAB Fourth Level Programming Language.

(Keywords: deflection of the vertical, hybrid model, Kriging interpolation, EGM 2008, geoidal undulation)

1. Introduction

Vertical deflection is a critical geodetic component and a physical property of the Earth's gravity field (Torge, Muller, and Pail, 2023). It reflects the relationship between geometric and physical quantities in our quest to map the Earth's surface. The deflection of the vertical, which

can be expressed in both meridian and prime vertical components, has previously been ignored in most geodetic computations (Featherstone, 1999). However, the integration of space-based geodetic positioning systems, such as the Global Navigational Satellite System (GNSS), with terrestrial-based positioning equipment, where orientation is defined by the Earth's gravity field, necessitates this critical component (Ogaja, 2022).

Space-based positioning systems are limited in areas where signal transmission is poor, such as in tunnels, indoor areas, or in areas with dense tree cover and high buildings (El-Rabbany, 2002). One way to address the limitation of space-based positioning is to combine a GNSS receiver with terrestrial equipment, e.g., a Total Station. This requires vertical deflection components to convert the geometric (ellipsoidal) coordinate derived from the GNSS system to the astronomical coordinate of the Total Station. Furthermore, the calibration of inertia sensors used in navigation requires accurate knowledge of the vertical deflection component (Hao et al., 2020). The deflection of the vertical is the angle between the gravity vector and the normal to the ellipsoid (Hofmann-Wellenhof and Moritz, 2006). It is typically represented in the prime vertical and meridian components. The deflection of the vertical offers important geophysical information regarding the Earth's underlying mass distribution as it reflects the variations in the Earth's mass density (Hofmann-Wellenhof and Moritz, 2006; Jonathan & Roger, 2012).

Astronomical observations were the first method used to determine vertical deflection (Thompson, 1978). Gravity measurements, often applying the Vening-Meinesz formula, are another approach for computing gravimetric vertical deflections (Torge, 2001; Agajelu, 2018). Soler, Carlson, and Evans (1989) developed a geometric model for calculating vertical deflection by integrating GNSS data and precise leveling (orthometric height). However, this method is suitable in regions with adequate, evenly distributed geodetic networks and known ellipsoidal and orthometric heights. Furthermore, traditional leveling operations, which are foundational to the geometric method, are often labour-intensive and time-consuming (Soler, Carlson, & Evans, 1989; Vandenberg, 1999). Vertical deflections are obtained from high-degree spherical harmonic models of the Earth's gravity field (e.g., EGM08, EGM96). This method is biased by truncation errors in the order and degree of the spherical harmonic coefficients (Jekeli, 1999). Global geoid models, such as EGM 2008, serve as first-order approximations of the Earth's surface but often fail to capture the finer details of the local terrain characteristics, resulting in spatial mismatches (Hart & Basil, 2023). These discrepancies highlight the need for localized corrections or enhancements to achieve greater accuracy in geoid modeling within specific regions.

In local geodetic networks, vertical deflections can be determined by combining GNSS observations with terrestrial measurements, such as zenith distances and horizontal and vertical angles (Vandenberg, 1999; Grafarend & Awange, 2000). However, as highlighted by

Vandenberg (1999), this method is marred by errors due to refraction in the measured zenith angles. Hirt, Burik, and Seeber (2010) used digital zenith cameras to determine vertical deflection components. This method requires precisely calibrated cameras and is also subject to refraction errors in zenith distance measurements. Similarly, Li and Jekeli (2008) explored the integration of Global Positioning System (GPS) and Inertial Navigation System (INS) vector gravimetric measurements to determine the vertical deflection. Furthermore, Sabri, Bambang, and Rina (2019) used terrestrial gravity disturbances and the derivative function of hostine to calculate vertical deflection in Semarang City, India.

Given the limitations of current models, this study proposes a new approach to determine the Earth's deflection of the vertical component using a hybrid model. The proposed hybrid model combines a geometric approach considered as highly accurate for estimating vertical deflection (Chiriac, 2017), with gravimetric techniques to offer a reliable result, especially in regions with limited geodetic control networks. The hybrid method capitalizes on widely available global geoid models and modifies them to fit local areas. Using orthometric height data from the local region, this approach calculates orthometric height differences between global and local domains to provide localized corrections. Surface interpolation algorithms then generate a correctional surface based on these corrections. The combination of this correctional surface with the global geoid model produces the so-called hybrid geoid model (Arana, Camargo, & Guimarães, 2017; Hart and Basil, 2023). Finally, integrating the hybrid geoidal undulation, which is the essentially the inverse of astro-geodetic height determination, gives the vertical deflection components (Merry & Vaníček, 1974).

The proposed hybrid model is easy to implement. It addresses the limitations of an inadequate geodetic network by combining the existing data with a global geoid model. The study demonstrates the successful application of this hybrid model in Rivers State, Nigeria, in that it showcases its potential to address regional geodetic challenges.

Section 2 provides an overview of the geometric and gravimetric methods used for calculating vertical deflection, which serve as the basis for the hybrid model. Section 2.2.3 presents a detailed description of the hybrid model and is followed by an explanation of the method of least squares estimation. The results of the study are presented in Section 3, and the conclusion is in Section 4.

2. Methodology

2.1. Study Area

The study area encompasses eight local government areas in Rivers State, Nigeria. It constitutes the Greater Port Harcourt City (GPHC), covering an area of about 10,900 square kilometres. Located between latitudes 04° 15′N and 04° 25′N and longitudes 05° 20′E and 07°

15′E, the region lies just north of the equator and east of the Greenwich Meridian. This area comprises the local governments of Port Harcourt, Oyigbo, Okrika, Ogu-bolo, Obio-Akpor, Ikwerre, Etche, and Eleme, which are among the 23 local governments in Rivers State. This work used the geodetic network established during the GPHC survey by Alcon. GPHC is a long-term project initiated by the Rivers State government to tackle the challenges of infrastructure and social decay caused by population growth. Within this region, there are four prominent higher education institutions: the University of Port Harcourt, Rivers State University, Rivers State College of Arts and Science, and Ignatius Ajuru University of Education. Additionally, the area has developed infrastructure, including a national airport, an international airport, two seaports, a game village, two integrated cultural centres, three multipurpose stadiums, and several national and international oil and gas companies. (Oba, 2015).

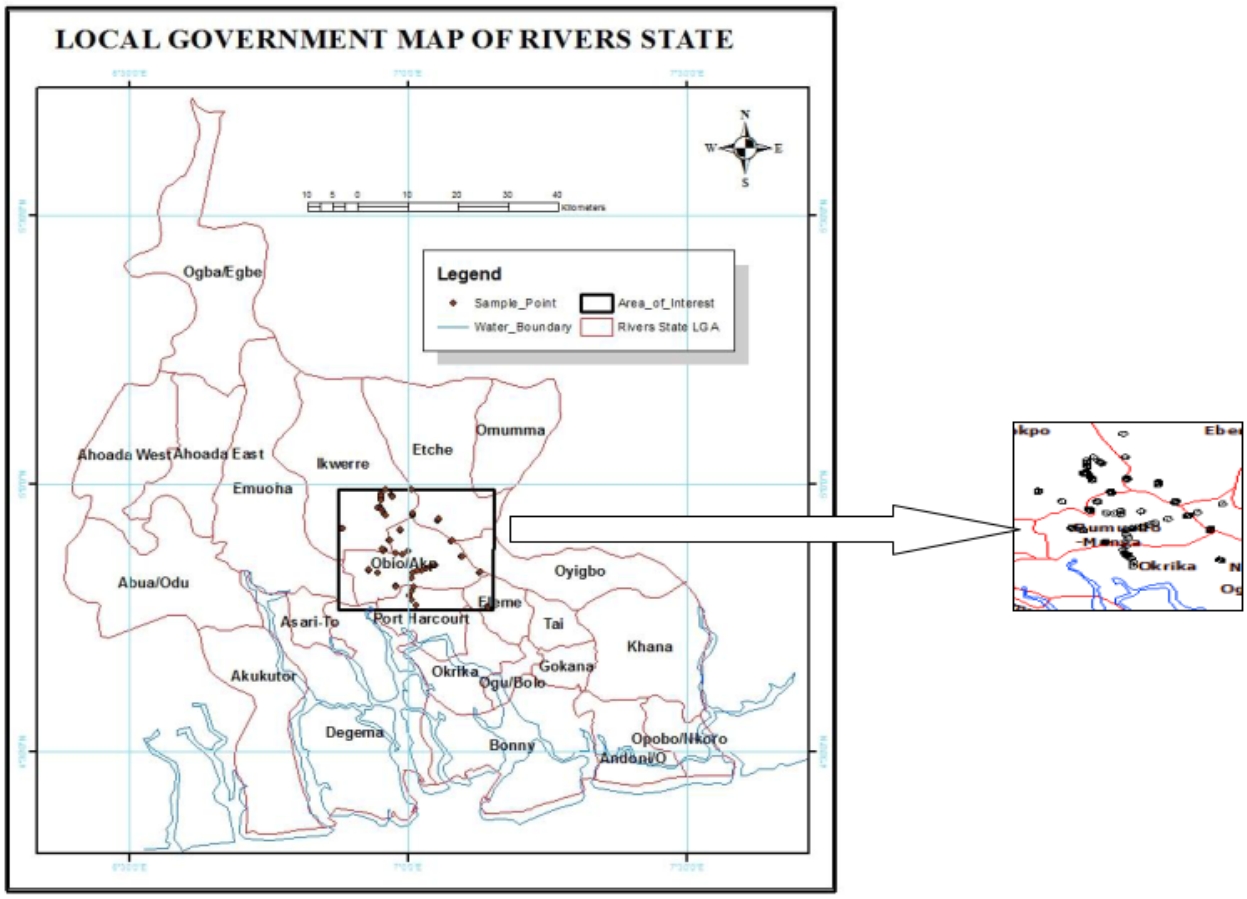

Figure 1: The study area (Source: Aleem, 2014).

2.2. Vertical Component Determination Methods

2.2.1. The Geometric Model

Soler, Carlson, and Evans (1989) proposed a geometric model to determine vertical deflection. The geometric model determines vertical deflection by differentiating the slope between the geoid and the ellipsoid. It assumes that the slope between the geoid and the ellipsoid is a linear function. This assumption is only true for a short baseline. For a long baseline, the slope between the geoid and the ellipsoid is no longer linear. As such, this model fails to account for such non-linearity. Hence, this model is suitable only in areas with dense geodetic networks and short baselines (Vandenberg, 1999; Basil *et al*., 2023). Knowing the slope between the ellipsoid and the geoid at the solution station allows for the calculation of the deflection of the vertical (ε) as described in Figure 2. The mathematical models that relate these quantities to vertical deflection components are discussed below.

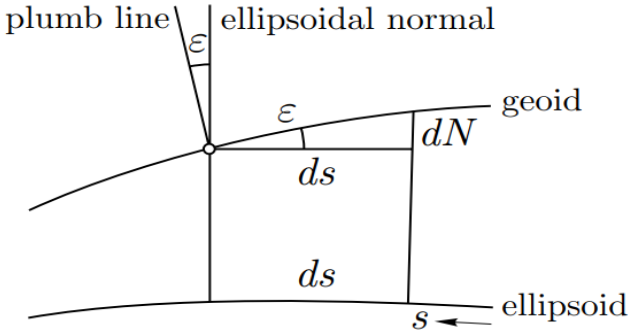

Figure 2: Schematic diagram showing the relationship between geoidal undulation and the vertical deflection (Source: Hofmann-Wellenhof and Moritz, 2006).

Figure 2 shows the relationship between the geoidal undulation (N) and the deflection of the vertical.(ε). The differential relationship between the geoid height (dN) and the deflection of the vertical (ε) is defined as given in equation (1) (Hofmann-Wellenhof and Moritz, 2006; Fubara et al., 2012; Agajelu, 2018):

$$\varepsilon = -\frac{dN}{dS} \quad \text{… eqn. (1)}$$

The deflection of the vertical of any geodetic azimuth (α) direction can be calculated using equation (2)

$$\varepsilon = \xi \cos\alpha + \eta \sin\alpha \quad \text{…eqn. (2)}$$

Substituting equation (2) in equation (1) gives equation (3):

$$-\frac{dN}{dS} = \xi.\cos\alpha + \eta.\sin\alpha \quad \text{… eqn. (3)}$$

For a detailed derivation of the geometric model, the reader should consult Ayhan (2009) and Basil *et al*., (2023).

2.2.2. The Gravimetric Model

The vertical deflection component can be determined from either the geopotential model of the Earth's gravity field (Jekeli, 1999), or the gravity disturbance using the hostine derivative function (Sabir *et al.,* 2019), or from gravity anomalies (Chiriac, 2017). The gravimetric determination of the deflection of the vertical from gravity anomaly is based on the Veining Meinesz integral given by Merry and Vanicek (1974); Hofmann-Wellenhof and Moritz (2006); Torge & Muller and Pail (2023); and Agajelu (2018), as given in Equations (4) and (5);

$$\xi = \frac{R}{4\pi\gamma}\iint_{\sigma}\Delta g(\psi,\alpha)\cos\alpha\,\frac{ds(\psi)}{d\psi}\sin\psi d\psi d\alpha \quad \text{… eqn. (4)}$$

$$\eta = \frac{R}{4\pi\gamma}\iint_{\sigma}\Delta g(\psi,\alpha)\sin\alpha\,\frac{ds(\psi)}{d\psi}\sin\psi d\psi d\alpha \quad \text{… eqn. (5)}$$

Where: ξ is the deflection component along the meridian, η is the deflection component along the prime vertical, R is the Gaussian mean radius of the earth, γ is the mean gravity of the Earth, Δg represents, gravity anomalies ψ is the spherical distance from the computation point to the particular gravity anomaly, and α denotes the azimuth of the line connecting the computation point with the point at which Δg is taken.

$$\frac{ds(\psi)}{d\psi} = -\frac{\cos\frac{\psi}{2}}{2\sin^2\frac{\psi}{2}} + 8\sin\psi - 6\cos\frac{\psi}{2} - 3\left(\frac{1-\sin\frac{\psi}{2}}{\sin\psi}\right) + 3\sin\psi\ln\left(\sin\frac{\psi}{2}+\sin^2\frac{\psi}{2}\right)$$

… eqn. (6)

$\frac{ds(\psi)}{d\psi}$ is the Veining Meinesz function.

The above equations (4) and (5) show how to calculate the vertical deflections from gravity anomalies. However, the calculation to determine the vertical deflection using the classical integral of the Veining Meinesz is tedious, time-consuming, and requires gravity data and large computer memory. Hence, for this study, the vertical deflection components were computed from EGM 2008 using Geoid Eval. The Earth Gravity Model (EGM) 2008 is complete to the spherical harmonics degree and order 2159 and contains additional coefficients extending to degree 2190 and order 2159 (Pelvis, Holmes, Kenyon & Cofactor, 2008).

The geoidal undulation implied by EGM 2008 ($N_{EGM\ 2008}$) can be obtained as given in equation (7);

$$N_{EGM} = \frac{GM}{r\gamma}\sum_{n=2}^{n\max}\left(\frac{a_{ref}}{r}\right)^n\sum_{m=0}^{n}\left(\ddot{C}_{nm}\cos m\lambda + S_{nm}\sin m\lambda\right)\ddot{P}_{nm}(\cos\vartheta) \quad \text{… eqn. (7)}$$

Where: GM is the product of the constant and mass of the earth, r is the geometric distance between the centre of the earth and the computation points, a_{ref} is a scaling parameter associated with a particular GGM (EGM 2008), $P_{nm}(\cos\vartheta)$ are fully normalized associated Legendre functions for degree n and order m, $\ddot{C}_{nm}$ and $\ddot{S}_{nm}$ are fully normalized spherical harmonic coefficients after reduction by the zonal harmonic of the reference ellipsoid, and n_{max} is the finite maximum degree of GGM (EGM 2008).

Heiskanen and Moritz (1967), Rapp (1981), Torge *et al.* (2023), and Agajelu (2018) are relevant studies detailing the computation of geoid undulations from geopotential models.

2.2.3. The Hybrid Model

Combining the geometric model and the gravimetric model is known as hybridization, resulting in a hybrid model (Arana, Camargo, and Guimaraes, 2017). The input data for the generation of a hybrid model are a GPS/leveling geoid height ($N_{geometric)}$ and a gravimetric geoid grid ($N_{EGM\ 2008}$). Hybridization is a process in three steps, as illustrated in Figure 3; first, the offsets of each GNSS/leveling point are computed using the EGM 2008 geoid model; second, a corrector surface is created; finally, this surface is fitted to the gravimetric geoid grid. The offsets calculated according to equation (8) are regarded as differences (ΔN) between the geometric and the gravimetric geoid model.

$$\Delta N = N_{geometric}(\vartheta,\lambda) - N_{EGM\,2008}(\vartheta,\lambda) \quad \text{… eqn. (8)}$$

However, a regular grid surface must be generated to combine the differences obtained with the geoid height derived from the geopotential model. This combined surface would serve as the base from which any interpolation for any point (location) would be determined, as shown in equation (9):

$$N_{Hybrud} = N_{EGM\,2008}(\vartheta,\lambda) + \Delta N(\vartheta,\lambda) \quad \text{… eqn. (9)}$$

The study calculated the deflection of the vertical component from the gradient of the developed hybrid geoid model, with the reference ellipsoid as a function of position according to equation (3). The refinement of the developed hybrid model is predicated on the generated correctional surface. The accuracy of this correctional surface is determined by the surface interpolation techniques used. For this reason, accurate surface representation is crucial for a precise hybrid geoid model. The researchers used two different surface representation techniques, including Inverse Distance Weighting (IDW) and Kriging, to generate the correctional surface and compare the results. As demonstrated by Basil and Hart (2023), the challenge with the IDW technique is the bull's-eye effect around the interpolation point, which introduces systematic bias in the correctional surface. Hence, we used the kriging interpolation technique in this study.

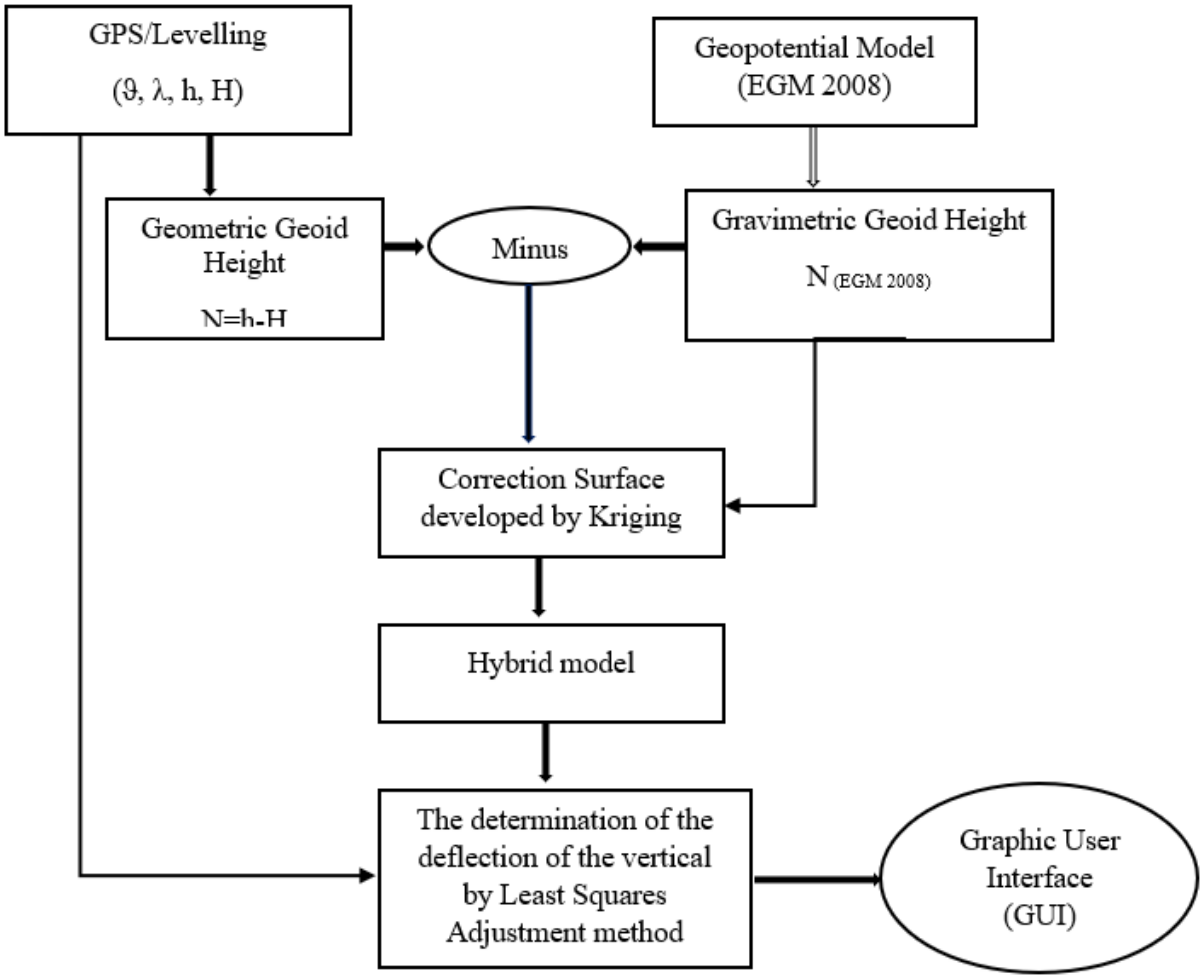

Figure 3: The process of integrating geometric and gravimetric methods

2.3. Surface Interpolation using Kriging Techniques

The Kriging technique is a set of statistical tools for modelling statistical relationships among measured points (using Kriging weights) to predict values and uncertainties for unmeasured locations. Kriging is a two-step process: first, the spatial covariance structure of the sampled points is determined by fitting a variogram; second, weights derived from this covariance structure are used to interpolate values for unsampled points or blocks across the spatial field. A variogram (sometimes called a semi-variogram) is a visual depiction of the covariance exhibited between each pair of points in the sampled data, which can be either a linear semi-variogram, a spherical semi-variogram, an exponential semi-variogram, or a power semi-variogram, the choice of which is fundamentally user-defined. The kriging weight for each interpolated point is calculated from the variogram, is based on the spatial structure of the data, and is applied to the sampled points according to equation (10) (Deutsch and Journal, 1992; Ogundere, 2018; Basil and Hart, 2023).

$$\hat{z}(x_i) = \sum_{j=1}^{n} \lambda_j z(x_j) \qquad \text{… eqn. (10)}$$

Where:

$\hat{z}(x_i)$ is the interpolated value,

λ_j is the kriging weight is determined from the semi-variogram.

$z(x_j)$ is the value of known sample points within the spatial field.

2.4. The Least Squares Method for Calculating Vertical Deflection

This study estimated the vertical deflection component using the observation equation method of least squares. According to Uotila (1978), Ayeni (2011), and Ogundere (2019), the following mathematical models, as given in equations (11 – 16), hold for a linear case of the observation equation model of least squares adjustment:

$$\hat{x} = \left(A^T PA\right)^{-1} A^T PL^b \quad \text{… eqn. (11)}$$

$$V = A\hat{x} + L^b \quad \text{… eqn. (12)}$$

$$\sigma_0^2 = \left(\frac{\mathrm{V^T PV}}{\mathrm{n-m}}\right) \quad \text{… eqn. (13)}$$

$$\sum \hat{X} = \sigma^{\circ}(A^T PA)^{-1} \quad \text{… eqn. (14)}$$

$$L^a = L^b + V \quad \text{… eqn. (15)}$$

$$\sum L^a = A \sum \hat{x} A^T \quad \text{… eqn. (16)}$$

Where: $\hat{x}$ is a vector of adjusted (unknown) parameters, V is the observation residual vector, L^b is a vector of original observations, and A is the design matrix. n is the number of observations, m is the number of unknown parameters, and n-m is the degree of freedom.

Equation (11) gives the unbiased least squares estimate, known as the Most Probable Value (MPV). Equation (12) gives the vector of residuals. Equation (13) gives the unit weight variance and tells us about the fitness of the adjustment model to the observation (Ayeni, 1981). It is known as the a-posterior variance. Equation (14) is the variance-covariance matrix, which is fundamentally important because the diagonal element yields the variance of the adjusted parameter, from which we can determine the standard deviation as a measure of the precision of the observation. We determined the adjusted observation from equation (15), with equation (16) representing the covariance matrix of the adjusted observation.

The study developed Design Matrix (A) using the functional model between the observed parameters ($\Delta H, \Delta h, \Delta S$ and α) and the unknown parameter (η and ξ) as given in equation (3).

$$A=\begin{bmatrix} \xi_1\cos\alpha_1 & \eta_1\sin\alpha_1 & 0 & 0 & . & . & . & 0 \\ \xi_1\cos\alpha_2 & \eta_1\sin\alpha_2 & 0 & 0 & . & . & . & 0 \\ 0 & 0 & \xi_2\cos\alpha_3 & \eta_2\sin\alpha_3 & 0 & . & . & 0 \\ 0 & 0 & \xi_2\cos\alpha_4 & \eta_2\sin\alpha_4 & 0 & . & . & . \\ . & . & . & . & . & . & . & . \\ . & . & . & . & . & . & . & . \\ . & . & . & . & . & . & \xi_{20}\cos\alpha_{40} & \eta_{20}\sin\alpha_{40} \\ 0 & 0 & 0 & . & . & . & \xi_{20}\cos\alpha_{41} & \eta_{20}\sin\alpha_{41} \end{bmatrix}_{(30\times45)}$$

It developed the matrix of observation as shown below.

$$L^b=\begin{bmatrix} -\frac{\Delta N_1}{\Delta S_1} \\ -\frac{\Delta N_2}{\Delta S_2} \\ . \\ . \\ . \\ . \\ -\frac{\Delta N_{40}}{\Delta S_{40}} \\ -\frac{\Delta N_{41}}{\Delta S_{41}} \end{bmatrix}_{(1\times45)}$$

The weight matrix is inversely proportional to the square of the distance in kilometres between the test station and the auxiliary station. MATLAB software served to facilitate the calculation process.

2.5. Data Acquisition

Secondary data, as presented in Table 1, were obtained from the Greater Port Harcourt City Development Authority (GPHA). The dataset includes geometric coordinates of geodetic controls acquired using a static GPS observation campaign, and precise orthometric heights from levelling carried out by ALCON Surveys. These activities comprised part of the mapping of Rivers State, Nigeria, initiated by the State Government in 2009 (Oba, 2015). Given the limited availability of data covering the study area, we visualized the acquired data using ArcGIS software. The study area was systematically divided into regular grids, as shown in Figure 4. From each grid, the positions of selected stations were extracted for further analysis. These positions were used to compute the gravimetric geoidal undulation based on the EGM 2008 model, as well as the geodetic distance and azimuth.

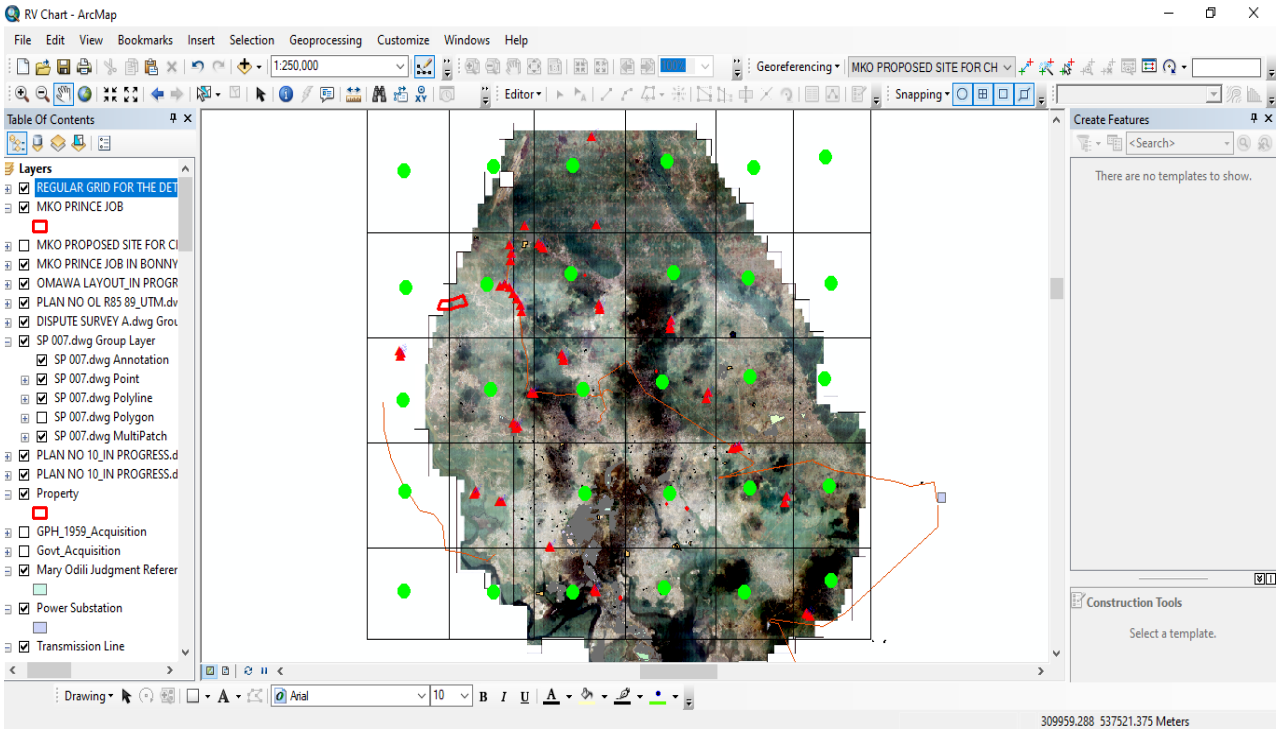

Figure 4: Gridding of the study area.

The red points in Figure 4 represent the common points, and the green points represent those whose gravimetric undulations were to be determined, respectively.

Table 1: Sample of the station coordinates of the geodetic network (GPHC, 2009)

STN	LAT. (ϑ) Decimal degree	LONG(λ) Decimal degree	East (m)	North (m)	Ellip. Height(m)	M.S.L. Height(m)
GPS001	5.0384	7.0027	278562.455	557256.887	47.654	29.513
GPS 02	4.98834	7.00544	278846.155	551710.235	42.542	24.294
GPS 03	4.97225	6.95118	272821.850	549949.018	38.771	20.630
GPS 04	4.98817	6.95968	273770.193	551706.979	41.357	23.096
GPS 05	4.97687	6.95053	272751.332	550460.253	39.485	21.289
GPS 06	4.96842	6.95077	272775.056	549525.528	38.351	20.218
GPS 07	4.95495	6.94708	272361.105	548036.898	34.627	16.476
GPS 08	4.95378	6.94428	272050.092	547908.448	36.819	18.648
GPS 09	4.97802	6.96892	274791.688	550581.147	38.155	20.165
GPS 10	4.97662	6.97037	274952.056	550425.802	39.661	21.445
GPS 11	4.97517	6.97196	275127.938	550264.880	40.589	22.342
GPS 20	4.8751	6.95599	273322.503	539201.795	32.335	14.017

2.6. Computation of Geodetic Distance and Azimuth

The determination of the geodetic curve distance and azimuth from the geodetic latitude and longitude defines the inverse problem of geometric geodesy (Fubara et al., 2014; Agajelu, 2018). Various mathematical models, such as the Puissant formulae, Gauss Mid-latitude formulae, Kivioja formula, and Vincenty's formula, have been developed for solving the direct and inverse problem of geometric geodesy (Thomson and Featherstone, 2005; Vincenty, 1975; Agajelu, 2018). The study employed Vincenty's inverse formula, implemented in the Australian online Geoscience software as shown in Figure 5, to compute the geodetic azimuth and distance between the networks. The results of the calculation, including the difference in heights between the various points (location) determined using Microsoft Excel 2013, are presented in Table 4.

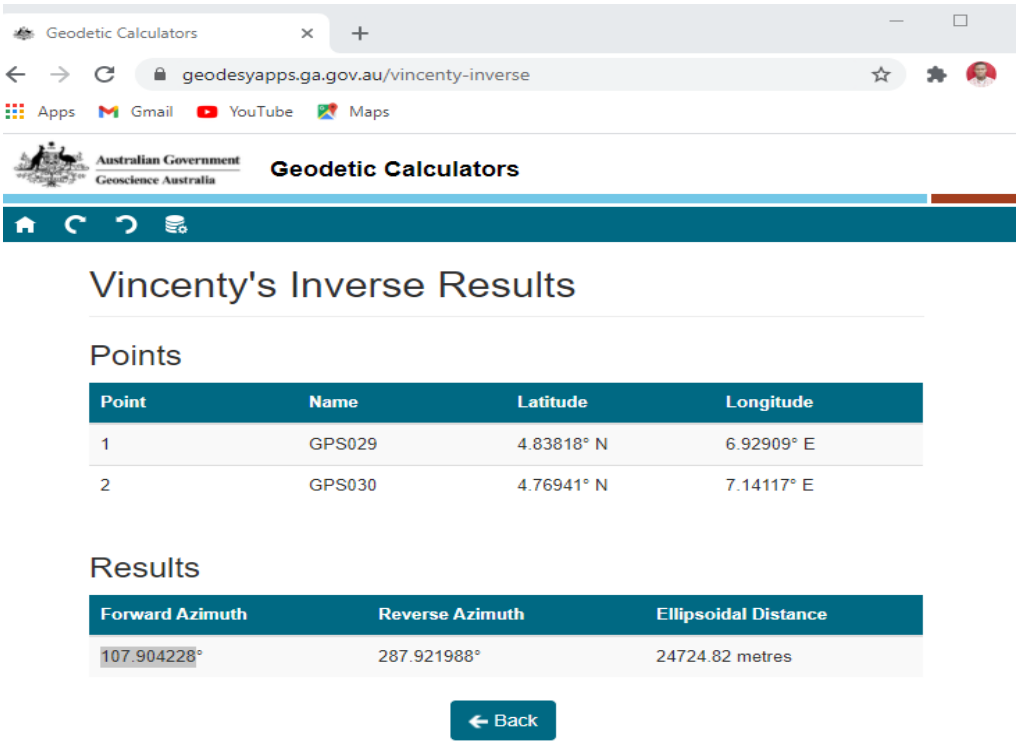

Figure 5: Australian Geoscience Software used for calculating the geodetic azimuth and ellipsoidal distances.

3. Results

Table 2 shows the results of the gravimetric geoid calculation and the difference between the two geoidal undulations, i.e., the difference between the GPS/levelling-determined geoid (geometric geoid) and the gravimetric geoidal undulation (EGM 2008 geoid). These discrepancies illustrate the localization error inherent in the global geoid model, which we addressed by generating a correctional surface through the kriging interpolation techniques.

This surface was combined with the gravimetric geoid model to create the hybrid geoid model (Hart and Basil, 2023).

Table 2: Differences between the geometric and the EGM-derived geoid height

Stations	LAT. (ϑ) Decimal degree	LONG.(λ) Decimal degree	Ellip. Height (m)	Orth. Height (m)	N=h-H (m)	EGM08 (m)	Diff. (m)
GPS 48	4.915312	6.983789	35.254	16.965	18.289	18.914	-0.625
GPS 49	4.807219	6.976287	29.336	10.995	18.341	18.975	-0.634
GPS 50	4.80699	6.977222	29.173	10.798	18.375	18.976	-0.601
GPS 51	4.781655	7.006075	28.033	9.558	18.475	19.018	-0.543
GPS 52	4.782322	7.005458	27.536	9.062	18.474	19.017	-0.543
GPS 53	4.783297	7.00524	27.441	8.824	18.617	19.016	-0.399
GPS 54	4.916897	6.880103	20.494	2.33	18.164	18.791	-0.627
GPS 55	4.916108	6.881155	20.982	2.819	18.163	18.792	-0.629
GPS 56	4.913982	6.880881	20.672	2.488	18.184	18.794	-0.61
						RMS	0.646636

3.1. Validation of the Developed Hybrid Model

As already established in geodetic literature, no interpolation method gives the exact representation of the modelled surface; however, the kriging interpolation method has the reputation of being a very precise and accurate interpolator (Ojigi, 2011; Basil and Hart, 2023). There is a need, therefore, to validate the developed hybrid geoid model to determine the degree of recoverability of the original value of the interpolated point (location). The validation involves determining the differences between a known point and an interpolated point (location). Five out of the 56 common points served to validate the developed hybrid model, and the result of the validation is presented in Table 3.

Table 3: Validation of the Hybrid Model. Here, Obs. is the difference between the geometric (ellipsoidal) height (h) from the GPS observation campaign, and the Orthometric height determined from the EGM 2008 model. The model values are those obtained from the hybrid geoid model generated using both kriging and IDW techniques. The differences (Diff.) between the Obs. values and the model values show the degree of recoverability and accuracy of the hybrid geoid model.

				Model Values (N)		Diff.	
SN	LAT. (ϑ)	Long. (λ)	Obs. (N=h-H)	Kriging Techniques	IDW Techniques	Kriging.	IDW
1	4.9559	7.15583	18.385	18.4212	18.412	-0.036	-0.027
2	4.8323	6.944122	18.273	18.2815	18.282	-0.009	-0.009
3	4.8072	6.97628	18.341	18.3731	18.373	-0.032	-0.032
4	4.8933	6.96628	18.314	18.2896	18.289	0.0244	0.025
5	4.7880	7.15629	18.488	18.4482	18.444	0.0394	0.0436
					RMS	0.0302	0.0295

Table 4: Geodetic Distances, Azimuths, and Geoidal Heights.

Solution Stations	LAT.	LONG.	N	Auxiliary Stations	LAT. (ϑ)	LONG.(λ)	N	Geodetic Dist. (S)	Geodetic Azimuth
GPS001	5.0384	7.0027	18.141	EGM 006	5.02659	7.15217	18.468	16626.58	94.49855
				GPS 036	4.89088	7.07611	18.396	18231.92	153.4741
				GPS004	4.98817	6.95968	18.261	7322.122	220.66083
EGM 005	5.02091	7.10648	18.4	EGM 001	5.01802	6.88276	18.125	24811.58	269.27177
				GPS 041	4.83205	7.12673	18.505	21005.29	173.85994
				GPS 050	4.80699	6.97722	18.375	27660.96	211.22318
EGM 008	4.96022	6.98963	18.278	EGM 001	5.01802	6.88276	18.125	13465.59	298.34235
				GPS 002	4.98834	7.00544	18.248	3569.851	29.41633
				GPS 027	4.83648	6.92827	18.269	15282.48	206.44676
EGM 009	4.961111	7.05541	18.349	EGM 018	4.83766	6.88402	18.256	23403.76	234.32409
				GPS 045	4.76837	7.14278	18.512	23413.73	155.54439
				EGM 004	5.02422	7.05017	18.269	7002.915	355.24024
EGM 010	4.95848	7.10319	18.423	GPS 016	4.93924	6.95796	18.215	16246.97	262.48154
				GPS 051	4.78165	7.00607	18.475	22324.52	208.85424
				EGM 001	5.01802	6.88276	18.125	25316.97	285.08356

The vertical deflection component was calculated using the least squares techniques employing the method of observation equation. MATLAB software was used to facilitate the calculation processes. The result of the computation is given in Table 5

Table 5: Vertical deflection components for fifteen stations within the study area

STN	LAT. (ϑ)	LONG. (λ)	North-South Comp. (ξ)	East-West Comp. (η)	Along the Normal (ε)
GPS001	5.0385	7.0027	0.0404 ± 0.0000412″	-0.0345″ ± 0.00003519″	0.077458″
EGM 005	5.0209	7.1065	0.0163″±0.00003505″	-0.0385″±0.00004709″	0.041808″
EGM 008	4.9602	6.9896	0.0314″±0.00003454″	-0.0288″±0.00005080	0.042608″
EGM 009	4.9611	7.0554	0.0259″±0.00002634″	-0.0308″±0.00006793″	0.040242″
EGM 010	4.9585	7.1032	0.0295″±0.00007031″	-0.0427″±0.00002789″	0.051899″
EGM 012	4.8892	6.8825	0.0086″±0.00003250″	-0.0367″±0.00005110	0.037694″
EGM 013	4.8952	6.9386	-0.0552″±0.00003475″	0.0069″±0.00004182″	0.05563″
EGM 014	4.8905	6.9974	0.0760″±0.00004253″	-0.2153″±0.00007022	0.22832″
SVG GPS 002	4.8001	6.9800	0.0416″±0.00007022″	0.009″±0.00005755″	0.042562″
EGM 019	4.8368	6.9990	-0.0286″±0.00002913″	-0.0423″±0.00003345″	0.051061″
EGM 020	4.8370	7.0530	0.0249″±0.00004389″	-0.0594″±0.0002433″	0.064408″
EGM 022	4.8414	7.1555	-0.0206″±0.00008639″	-0.0085″±0.00005584″	0.022285″
GPS053	4.7833	7.0052	0.0711″±0.0000002997″	-0.0351″±0.0002725″	0.079292″
EGM 027	4.7816	7.1009	0.0181″±0.0003487″	-0.0469″±0.0009024″	0.050271″
EGM 028	4.7880	7.1563	0.0748″±0.0005223″	0.0270″±0.0003370″	0.079524″

The a-posterior variance is given as:

$$\sigma^2 = \left(\frac{V^T PV}{n-m}\right) = 0.000005693''$$

The a-posterior standard error is given as:

$$\sigma = \sqrt{\left(\frac{V^T PV}{n-m}\right)} = \pm 0.0000453''$$

3.2. Comparison between the Geometric, Hybrid, and the EGM 2008 derived vertical deflection components

To evaluate the accuracy of the hybrid model, vertical deflection components were also determined using the geometric method and the EGM 2008 geopotential model for a single point (location) within the study area. The results are presented in Table 6 and Figure 6.

Table 6: Comparison of the vertical deflection components values obtained from geometric method, hybrid method, and geopotential model (EGM 2008).

Comparison of the deflection of the vertical				
Methods	North-South Component (ξ)	East-West Component (η)	difference	
Geometric Method	0.0473″	-0.0393″	ξ	η
Hybrid Model	0.0404″	-0.0345″	0.0069	-0.0048″
EGM 2008	0.0157″	-0.0246″	0.0316	-0.0147″

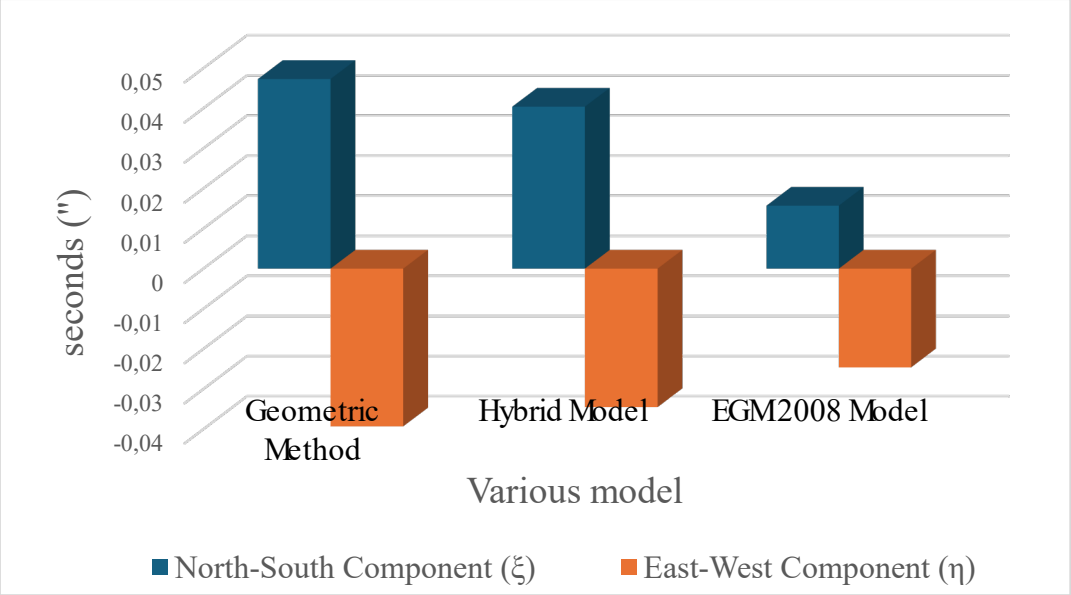

Figure 6: Comparison of the vertical deflection components as determined by the geometric method, hybrid model, and EGM between the components of the deflection of the vertical derived using the geometric method, the hybrid method, and the gravimetric method.

The vertical deflection map for the study is presented in Figure 6. Surfer 13 software, based on the kriging gridding techniques, was used for this purpose.

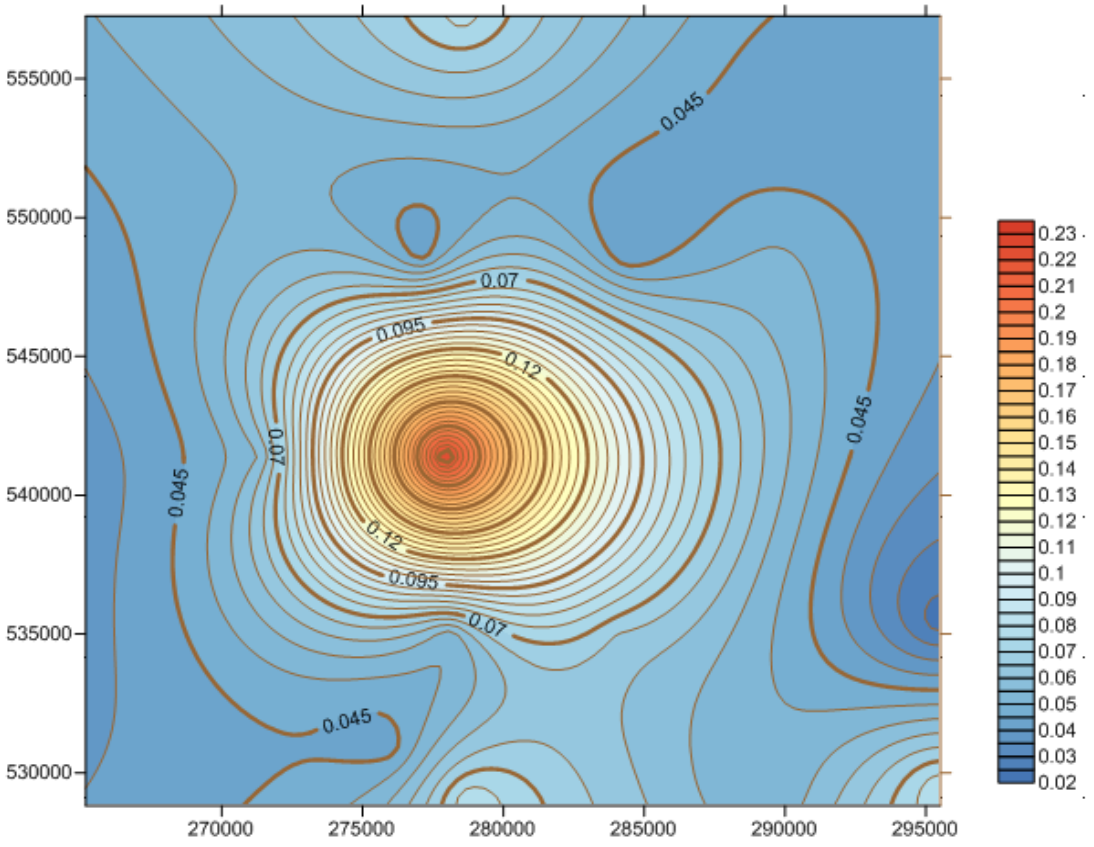

Figure 7: Map showing the total vertical deflection of the vertical values within the study area.

3.3. Discussion of Results

Table 1 presents a comparison between the geometric geoid undulation and the gravimetric geoid undulation as calculated from the geopotential model (EGM 2008), with a root mean square of 0.6466. Using the hybridization, the study found that the root mean deviation between the hybrid model and the geometric model was 0.0302 for kriging and 0.0295 for IDW. This shows the degree of fitness of the developed hybrid model compared to the geometric model. Irrespective of the fact that IDW gives a smaller RMS, it generates concentric circles around the interpolation point, usually referred to as the bull's-eye effect (Hart and Basil, 2023; Ogiji,2011). The kriging technique gives a minimum variance estimate by minimizing the sum of the weighted residuals; that is, it gives an unbiased estimate of the interpolated point and is more reliable than the IDW interpolation technique.

The vertical deflection component estimated using the hybrid model as described in this research is within the range of -0.0552″ to 0.0784″ in the north-south component and -0.05940″ to 0.21530″ in the east-west component. This is shown in Table 3, with a posterior standard error of $\pm 0.0000453''$. The small variations in the vertical deflection component with respect to position reflect the internal distribution of the Earth's mass density, which portrays the relative flatness of the terrain characteristic.

As seen in Table 5, the vertical deflection components obtained from the developed hybrid model fit reasonably well with those obtained using the geometric method, as opposed to the gravimetric deflection of the vertical computed from the geopotential model (EGM 2008): there was a difference of 0.0069″ and -0.0048″ in the north-south and east-west components, respectively. Hence, the hybrid model can be considered the best alternative to the geometric method for determining vertical deflection components in areas served by poor geodetic infrastructure and unevenly spaced geodetic networks. The difference between the geometrically derived vertical deflection component and that derived from the geopotential model (EGM 2008) shows the fitness of the EGM 2008 model with respect to the local gravity field of the study area. This further demonstrates the use of vertical deflection in assessing the fitness of a particular geoid model.

4. Conclusion

This research highlights the effectiveness of the hybrid model for computing the vertical deflection component in Rivers State, Nigeria. The proposed approach integrates both geometric and gravimetric methods through the application of a surface interpolation algorithm. The findings demonstrate that the hybrid model aligns well with the geometric method, making it a viable solution for regions with sparsely distributed geodetic networks.

The accuracy of the hybrid vertical deflection component is strongly influenced by the surface interpolation algorithm and the density of the common sample points used. Thus, increasing the number of common points would improve the accuracy of the vertical deflection components.

To further improve the reliability and applicability of the hybrid model, it is recommended to expand the network of geodetic sample points across the study area and other similar regions. Additionally, exploring advanced interpolation techniques and integrating high-resolution global gravity models could further refine the accuracy of the vertical deflection component. Future studies should also consider testing the model's performance in diverse geodetic and topographic conditions to establish its broader applicability.

Acknowledgement

The authors gratefully acknowledge the Office of the Surveyor General of Rivers State and the Greater Port Harcourt City Council, Nigeria, for providing the geodetic network data of Rivers State used in this study. Special thanks are also extended to the staff of the Department of Surveying and Geomatics, Rivers State University, particularly Surveyor Oba Tamunobelema, for the insightful discussions during this study. The authors also appreciate the valuable comments and suggestions from the three anonymous reviewers, which have significantly contributed to improving the quality of this manuscript.

5. REFERENCE

Agajelu S.I. (2018). Geodesy: The Basic Theories-Classical and Contemporary, EL'DEMAK Publishing, 76 Robinson Street, Uwani, Enugu, ISBN 978-978-8436-99-0.

Aleem A. (2014). Adaptation of the Global Orthometric Model to the Local Geoid Model using the Satlevel Collocation Techniques. PhD Thesis, Department of Surveying and Geoinformatics, University of Lagos, Nigeria.

Arana D., Camargo P. O., & Guimaraes G. N. (2017). Hybrid Geoid Model: Theory and Application in Brazil. Annals of Brazilian Academy of Sciences vol. 89(3). ISSN: 1678-2690.

Ayeni O. O., (2011). An Investigation into the Choice of the Most Appropriate Least Squares Method for Position Determination. F. A. Fajemirokun (Ed). Contemporary Issues in Surveying and Geoinformatics. Published by BPrint, 51, Remi-Fani Kayode Avenue, off Oduduwa Street, GRA Ikeja, Lagos, Nigeria. ISBN: 978-915-670-2.

Ayeni, O. O. (1981). Statistical Adjustment and Analysis of Data (with applications in geodetic surveying and photogrammetry, a Manual. Department of Surveying & Geoinformatics, Faculty of Engineering, University of Lagos, Nigeria.

Ayhan, C. (2009): Determination of the Deflection of Vertical Components via GPS and Levelling Measurement: a Case Study of a GPS Test Network in Konya, Turkey. Scientific Research and Essay Vol 4 (12), 1438-1444, December 2009. Available online at http://www.academicjournals.org/SRE.

Basil D. D., Hart L., Jackson K. P., and Oba T. (2021). Determination of Deflection of the Vertical Components: Implications on Terrestrial Geodetic Measurement. World Journal of Geomatics and Geosciences. vol.1(1), 34-49, DOI: 10.31586/wjgg.2021.104.

Bernhard Hofmann-Wellenhof and Helmut Moritz (2006). Physical Geodesy.2nd Edition. Springer-Verlag Wien, New York. ISBN: 13 978-3-211-33544-4.

Chiriac V., (2017). Study of Deflection of the Vertical Determination Methods and the Influence on Traditional Terrestrial Three-dimensional Geodetic Measurements.

Deutsh C. V., & Journal A. G. (1992). GSLIB- Geostatistical Software Library and Users Guide, Oxford University Press, New York.

El-Rabbany A. (2002). Introduction to GPS: The Global Positioning System. Artech House Inc. 685 Cantoon Street, Norwood, MA 02062. ISBN: 1-58053-183-1

Fubara M. J., Fajimirokun F. A., Ezeigbo, (2014). Fundamentals of Geodesy. Concept Publication Limited. 77, Shipeolu Street, Palmgrove, Lagos, Nigeria. ISBN: 978-987-525562-1-5.

Ghilani C. D. & Wolf P. R. (2006). Adjustment Computations; Spatial Data Analysis. Published by John Wiley & Sons, Inc., Hoboken, New Jersey, 4th ed. ISBN-13-978-0-471-69728-2.

Grafarend, E.W. and Awange, J. L. (2000). Determination of Vertical Deflections by GPS /LPS measurements.*ZeitschriftfürVermessungswesen,* 125(8), 279-288.

Hao S., Zhang Z., Zhou Z., Zhou J., Chang Z., and Xu Z. (2020). Analysis of Deflection of Vertical for Compensation of Inertia Navigation System. Hindawi Mathematical Problems in Engineering. (Available from: https//doi.org/10.1155/2020/1975672.

Hart, L., and Basil D. D. (2023). Comparison of Three Selected Interpolation Techniques for Hybrid Geoid Determination in Rivers State, Nigeria. *Nigerian Journal of Environmental Sciences and Technology*. Vol. 7 (1).

Heiskanen W. A. and Moritz H. (1967). Physical Geodesy. W. H. Freeman and Company, San Francisco. ISBN: 978-3-211-33535-1.

Hirt, C., Bürki, B., Somieski, A., and G. Seeber (2010): Modern Determination of Vertical Deflections using Digital Zenith Cameras. *Journal of Surveying Engineering* 136(1), Feb, 2010, 1-12 DOI: 10.1061/_ASCE_SU.1943-5428.0000009.

Jekeli C. (1999). An Analysis of Vertical Deflections derived from a High Degree Spherical Harmonic Model. *Journal of Geodesy*, Springer-Verlag.

Merry C. L., and Petre Vanicek (1974). A method of Astrogravimetric Geoid Determination. Technical Report No. 27, Department of Surveying and Engineering, University of New Brunswick, Fredericton, N.B., Canada.

Ogaja C. A. (2022). Introduction to GNSS Geodesy: Foundation for Precise Positioning using the Global Navigation Satellite System. Springer Nature Switzerland. ISBN: 978-3-030-91820-0.

Ogundere J. O. (2019). Understand Least Squares Estimation and Geomatics Data Analysis. John Wiley & Sons, Inc., 111 Rivers Street, Hoboken, NJ 07030, USA. ISBN: 9781119501442.

Ojigi M. L. (2011). Determination of Suitable Terrain Surface Modelling Algorithms for the Hydraulic Design of Storm Sewers. As in Fajimirokun F. A. Ed. (2011). *Contemporary issues in Surveying and Geoinformatics*. Published by Bprint 51, Remi-FaniKayode Avenue, off Oduduwa Street, GRA Ikeja, Lagos. ISBN: 97 8-915-670-2.

Rapp, R. H. (1991). Lecture notes on Geometric Geodesy Part I. Department of Geodetic Science and Surveying, The Ohio State University, 1958 Neil Avenue, Columbus, Ohio, 43210.

Sabri L. M., Bambang S., & Rina D. I., (2019). Determination of the vertical deflection based on Terrestrial Gravity Disturbance Data (a Case Study in Semarang City). A Conference Paper

presented at the First International Conference on Geodesy, Geomatics, and Land Administration. KnE Engineering, 106-114.

Soler T, Carslon A. E & Evans A. G. (1989). Determination of Vertical Deflections Using the Global Positioning System and Geodetic Levelling, *Geophysical Research. Latter.* 16(7): ISSN: 695 698.

Thomas C. M., and Featherstone W. E. (2005). Validation of Vincenty's Formulas for the Geodesic using a New Fourth-order Extension of Kivioja's Formula. *Journal of Surveying Engineering*, vol. 131(1), ©ASCE, ISSN 0733-9453/2005/1 20–26.

Torge W., Muller J., and Pail R. (2023). Geodesy.5th Edition. De Guyter, Berlin, New York. ISBN: 978-3-11-020718-7.

Uotila U. A., (1967). Introduction to Adjustment Computations with Matrices; Lecture notes (unpublished), Geodetic Science Department, the Ohio State University.

Vandenberg D. J. (1999). Combining GPS and Terrestrial Observations to determine Deflection of the Vertical. A Thesis submitted to the Faculty of Purdue University.

Vincenty T. (1975). Direct and Inverse Solutions of Geodesics on the Ellipsoid with Application of Nested Equations" (Available from http://www.ngs.noaa.gov/PUBS_LIB/inverse.pdf)